

# Neural Temporal Point Process for Forecasting Higher Order and Directional Interactions

Tony Gracious, Arman Gupta, Ambedkar Dukkipati

Department of Computer Science and Automation, Indian Institute of Science Bangalore

{tonygracious, armangupta, ambedkar}@iisc.ac.in

## Abstract

Real-world systems are made of interacting entities that evolve with time. Creating models that can forecast interactions by learning the dynamics of entities is an important problem in numerous fields. Earlier works used dynamic graph models to achieve this. However, real-world interactions are more complex than pairwise, as they involve more than two entities, and many of these higher-order interactions have directional components. Examples of these can be seen in communication networks such as email exchanges that involve a sender, and multiple recipients, citation networks, where authors draw upon the work of others, and so on. In this paper, we solve the problem of higher-order directed interaction forecasting by proposing a deep neural network-based model *Directed HyperNode Temporal Point Process* for directed hyperedge event forecasting, as hyperedge provides native framework for modeling relationships among the variable number of nodes. Our proposed technique reduces the search space of possible candidate hyperedges by first forecasting the nodes at which events will be observed, based on which it generates candidate hyperedges. To demonstrate the efficiency of our model, we curated four datasets and conducted an extensive empirical study. We believe that this is the first work that solves the problem of forecasting higher-order directional interactions.

## 1 Introduction

Networks or graphs are the default abstraction for modeling real-world interactions between entities. Here, nodes represent entities, and edges represent interaction. However, most real-world interactions involve a group of entities, and many of these interactions have directional nature [Kim *et al.*, 2022], where one set of entities interacts with another set. The ability to predict these interactions has important applications in blockchain [Ranshous *et al.*, 2017], recommendation systems [Liu *et al.*, 2018], and so on. In our work, we focus on the problem of forecasting these higher-order directed interactions as hyperedges formation in a directed hypergraph.

A directed hypergraph can be represented as  $\mathbf{H} = (\mathcal{V}, \mathcal{H})$ . Here,  $\mathcal{V} = \{v_1, \dots, v_{|\mathcal{V}|}\}$  is the set of nodes and  $\mathcal{H} = \{h_1, \dots, h_{|\mathcal{H}|}\}$  is the set of hyperedges. In this hyperedge  $h = (h^r, h^l) \in \mathcal{H}$  represents a relation between two sets of nodes with  $h^r \subset \mathcal{V}$  as the right hyperedge and  $h^l \subset \mathcal{V}$  as the left hyperedge. For modeling higher-order interaction, each  $h \in \mathcal{H}$  is associated with a timestamp  $t_i$  indicating the time at which the interaction occurred. In figure 1, we show an example of directed higher-order interactions  $\{(h_1, t_1), (h_2, t_2), (h_3, t_3)\}$  emerging in a citation network between authors of a paper and authors of papers referred by them. Earlier works [Trivedi *et al.*, 2019; da Xu *et al.*, 2020; Liu *et al.*, 2022; Cao *et al.*, 2021] in interaction forecasting use graph neural network based techniques to learn dynamic representations/embeddings for nodes that are then used for downstream tasks like link prediction, node classification, and so on. These representations are trained by supervised information provided by type and time of future interactions. However, earlier methods are developed for forecasting pairwise interactions and can be applied to learn representation from hyperedge events only by projecting them to pairwise interaction. However, this will lead to information loss, as shown in [Gracious and Dukkipati, 2023]. Also, [Benson *et al.*, 2018] has demonstrated that pairwise models cannot distinguish between temporal motifs like open triangles and closed triangles emerging in a temporal network.

Recent work [Gracious and Dukkipati, 2023] used the temporal point process (TPP) for hyperedge type prediction for modeling higher-order interaction. However, this method is developed for undirected and bipartite hyperedges, which only show a single type of relations. Unlike these, a directed hyperedge can represent three types of relations. For example, consider a directed higher-order interaction  $((v_1, v_2), (v_3, v_4))$ , an undirected hyperedge model will show relations  $\{(v_1, v_2), (v_2, v_3), (v_1, v_3), (v_1, v_4), (v_2, v_4), (v_3, v_4)\}$ , these are the self connections in an undirected hyperedge, and a bipartite hyperedge model will show  $\{(v_1, v_3), (v_1, v_4), (v_2, v_3), (v_2, v_4)\}$ , these are cross-connection between left and right hyperedges. However, a directed hyperedge will show relations between self-connection in right hyperedge  $\{(v_1, v_2)\}$ , self-connection in left hyperedge  $\{(v_3, v_4)\}$ , and cross connection between left and right hyperedge,  $\{(v_1, v_3), (v_1, v_4), (v_2, v_3), (v_2, v_4)\}$ .

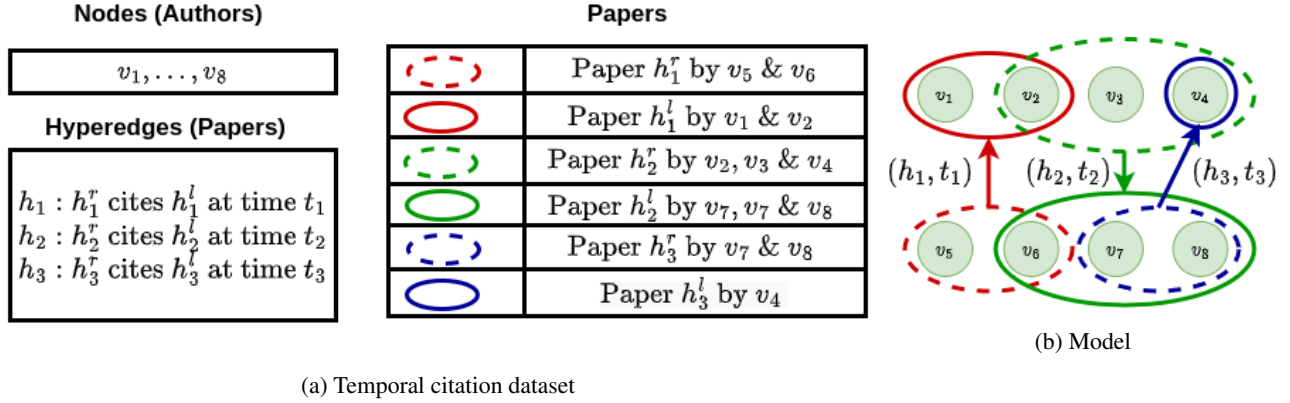


Figure 1: A temporal citation network modeled as a directed hypergraph event graph with 8 nodes and 3 hyperedges. Here,  $t_3 > t_2 > t_1$ .

Further, [Gracious and Dukkipati, 2023] will not scale well for forecasting events as the number of candidate hyperedges is of exponential order to the number of nodes. For example, to predict future links in directed graphs with nodes  $\mathcal{V}$ , one need to compare all the  $^{|\mathcal{V}|}P_2$  pairwise combinations of nodes in the network. However, to forecast directed hypergraphs, there are a maximum of  $2^{|\mathcal{V}|}$  combinations of nodes in the left and right hyperedges. Another limitation is that it uses a continuous time RNN in a representation learning framework that updates its dynamic node embedding after each interaction. It will affect the model’s scalability to apply to datasets with many interactions, as we cannot do batch training. The other recent works [Benson *et al.*, 2018; Liu *et al.*, 2022] on hyperedge forecasting focused only on modeling interaction between three nodes.

Our model *Directed HyperNode Temporal Point Process* **DHyperNodeTPP** tries to address the abovementioned issues to create a scalable hyperedge forecasting model. Unlike previous models that forecast future interactions by defining TPP on hyperedges, we use TPP on nodes to predict nodes that will observe events, which can be done in  $O(|\mathcal{V}|)$  operations. Then we group those nodes that observe concurrent events and use them to create candidate hyperedges for interaction prediction models. Further, for scalable training, we use a message-passing framework where we store the features of interactions of each node and then use them to update the node embeddings before the next batch. This is achieved by using a memory module to store the node embeddings and a recurrent neural network to update the node based on its messages. In addition to that, we provide a novel architecture for directed hyperedge prediction by combining the three levels of relationships involved in it. The following are the main contributions of our work. **1)** A temporal point process model for forecasting directed hyperedges in a scalable way; **2)** A scalable dynamic representation learning approach that uses temporal graph attention networks; **3)** A directed hyperedge prediction model; **4)** Creation of four real-world directed higher-order interaction datasets from open-source data; **5)** Extensive experiments showing the advantage of our model on event forecasting over existing modeling techniques.

## 2 Related Works

### 2.1 Learning with Hypergraphs

The interest in extracting information from higher-order relational networks started with the seminal work of [Zhou *et al.*, 2006] that extended the spectral clustering algorithm for pairwise graphs to hypergraphs. This was followed by works of [Ghoshdastidar and Dukkipati, 2017] that proved the consistency of clustering algorithms. Further, statistical models [Stasi *et al.*, 2014; Ng and Murphy, 2021] try to partition the nodes of hypergraph into clusters through maximum likelihood estimation of their parameters. Coordinated matrix minimization (CMM) [Zhang *et al.*, 2018] used non-negative matrix factorization for link prediction in hypergraphs. However, deep learning approaches have only recently been developed for building models on Hypergraphs. Hypergraph neural networks (HGNN) [Feng *et al.*, 2019] and HyperGCN [Yadati *et al.*, 2019] used the clique expansion of hypergraphs to convert it to pairwise graphs and use graph convolution operations to learn node embeddings for supervised and semi-supervised node classification problems. Further, for the same tasks [Bai *et al.*, 2021] defined graph convolution and attention operations directly using the incidence matrix of the hypergraphs. However, collecting supervised information is difficult as it is time-consuming and costly. So, the recent works Hyper-SANN [Zhang *et al.*, 2020] and NHP [Yadati *et al.*, 2020] use hyperlink prediction based methods to extract higher-order interaction information available in the form of link information and click data. However, all these methods focus on learning information from the static graph and ignore the temporal information.

### 2.2 Dynamic Link Forecasting

The early works in dynamic link forecasting focused only on pairwise edge prediction. This involves discrete time models like DySAT [Sankar *et al.*, 2020] and NLSM [Gracious *et al.*, 2021], which discretize the time into snapshots and predicts edges in the following snapshot. Our method focuses on building continuous time models since discretization involves information loss and requires domain knowledge. Jodie [Kumar *et al.*, 2019] and TGAT [da Xu *et al.*, 2020] use continuous time models by learning a functional form for modeling

temporal drift. Even though they can predict the presence of an edge at a particular time, they cannot estimate the time at which interaction will occur. The temporal Point Process is a popular framework for modeling dynamic networks that can do both. DyRep [Trivedi *et al.*, 2019] and DSPP [Cao *et al.*, 2021] use the temporal point process to model the time distribution of edge formation. Note that none of these above-mentioned works can model higher-order interactions available abundantly in the real world. The importance of higher-order analysis is empirically shown in the work of [Benson *et al.*, 2018]. They focused on the problem of higher-order interactions between three nodes, mainly on the issue of distinguishing between the formation of the open triangle and close triangle interactions. This was further extended to a deep learning framework by [Liu *et al.*, 2022]. They were able to model the time occurrence of different types of interaction by using neural network-based modeling techniques. The problem of hyperedge forecasting using a temporal point process framework has been addressed in recent work by [Gracious and Dukkipati, 2023]. However, their work ignores the scalability issues and direction information in the interactions.

### 3 Model

#### 3.1 Problem Definition

The goal of our work is to learn a probability distribution over the event type ( $e_{n+1}$ ) and the time ( $t_{n+1}$ ) of the next event given the history,  $p((e_{n+1}, t_{n+1})|\mathcal{E}(t_n) = \{(e_0, t_0), \dots, (e_n, t_n)\})$ . Here,  $e_n = \{h_{n,m}\}_{m=0}^{L_n}$  represents the  $L_n$  concurrent higher-order interactions occurring at time  $t_n$ ,  $h_{n,m} = (h_{n,m}^r, h_{n,m}^l)$  with  $h_{n,m}^r \subset \mathcal{V}$  and  $h_{n,m}^l \subset \mathcal{V}$  is  $m$ th interaction at time  $t_n$ ,  $n$  is the index of the event and  $m$  is the index of the concurrent event. Unlike previous works on higher-order interaction forecasting, we use batch training using a memory module to store the dynamic node embeddings. These embeddings are updated by a recurrent neural network module using the stored interaction features in the form of messages from the previous batch. Through this, we can apply parallel training techniques and make our model scalable to real-world datasets involving millions of interactions. We divide future forecasting into two tasks, as shown in Figure 2. The first task is to identify the nodes where future events will occur, and the second is to predict the types of hyperedge interactions occurring within these nodes.

#### 3.2 Event Modeling on Nodes

Given the history,  $\mathcal{E}(t_n)$ , the goal of node event modeling is to forecast time and nodes at which events will occur,  $(\cup e_{n+1}, t_{n+1})$ . Here,  $\cup e_{n+1} = (\cup e_{n+1}^r = \cup_{m=0}^{L_n} h_{n+1,m}^r, \cup e_{n+1}^l = \cup_{m=0}^{L_n} h_{n+1,m}^l)$  is the set of all the nodes, where an interaction event is observed at time  $t_{n+1}$  in the right and left hyperedge. We model the event time for a node using exponential distribution, so for a node,  $v_i$  event time follows  $t \sim \mu_i \exp\{\mu_i t\}$ . Here,  $\mu_i > 0$  is the rate parameter of an exponential distribution, and it is parameterized by a neural network that takes node embedding of  $v_k$  at time  $t_n$  as the input. So, for node  $v_i \in h_{n+1,m}^r$  the rate parameter is,

$$\mu_{n+1,i}^r = \exp\{\mathbf{W}_t^r \mathbf{v}_i(t_n)\}. \quad (1)$$

Here,  $\mathbf{W}_t^r \in \mathbb{R}^{d \times 1}$  is a learnable parameter and  $\mathbf{v}_i(t_n) \in \mathbb{R}^d$  is the node embedding of  $v_i$  in the right hyperedge ( $h_{n,m}^r$ ) at time  $t_n$ . Similarly, we will model node events for nodes present in the left hyperedge ( $h_{n,m}^l$ ). The complete likelihood for the next event on nodes in  $e_{n+1}$  at time  $t_{n+1}$  can be expressed as,

$$p((\cup e_{n+1}, t_{n+1})|\mathcal{E}(t_n)) = \prod_{v_i \in \cup e_{n+1}^r} \mu_{n+1,i}^r \prod_{v_i \in \cup e_{n+1}^l} \mu_{n+1,i}^l \prod_{i=1}^{|V|} \exp\{\mu_{n+1,i}^r(t_{n+1} - t_n)\} \exp\{\mu_{n+1,i}^l(t_{n+1} - t_n)\}. \quad (2)$$

Here,  $\exp\{\mu_{n+1,i}^r(t_{n+1} - t_n)\}$  is the probability that the event was not observed on node  $v_i$  after  $t_n$  till time  $t_{n+1}$ , and  $\mu_{n+1,i}^r$  is the rate of an event for node  $v_i$ . The next event time for each node can be estimated using the property of exponential distribution,  $\mathbb{E}[t_{n+1} - t_n] = \frac{1}{\mu_{n+1,i}^r}$ . Similarly, we will estimate the event time for nodes present in the left hyperedge. For directed hyperedge forecasting, we find the nodes that have the minimum event time and use them to generate candidate hyperedges for the hyperedge prediction module in the following section.

#### 3.3 Hyperedge Prediction

Given that events are observed in the following nodes  $\cup e_{n+1}$  at time  $t_{n+1}$ , generate all the possible hyperedge candidates  $\tilde{\mathcal{H}}_{n+1}$  from them and assign each one of them a label  $y_{\tilde{h}_{n+1,m}} \in \{0, 1\}$ , here,  $y_{\tilde{h}_{n+1,m}} = 1$  if  $\tilde{h}_{n+1,m}$  was observed if not 0. Then the probability of observing  $e_{n+1}$  at time  $t_{n+1}$  is,

$$p(\tilde{\mathcal{H}}_{n+1}, \mathcal{Y}_{n+1}|\mathcal{N}_n, t_{n+1}, \mathcal{E}(t_n)) = \prod_{\tilde{h}_{n+1,m} \in \tilde{\mathcal{H}}_{n+1}} \sigma(\lambda_{\tilde{h}_{n+1,m}}(t_{n+1}))^{y_{\tilde{h}_{n+1,m}}} (1 - \sigma(\lambda_{\tilde{h}_{n+1,m}}(t_{n+1})))^{1 - y_{\tilde{h}_{n+1,m}}}. \quad (3)$$

Here,  $\sigma(x) = \frac{1}{1 + \exp(-x)}$ ,  $\mathcal{Y}_{n+1} = \{y_{\tilde{h}_{n+1,m}}\}_{\tilde{h}_{n+1,m} \in \tilde{\mathcal{H}}_{n+1}}$ ,  $\mathcal{N}_n = (\mathcal{N}_n^r, \mathcal{N}_n^l)$  is the tuple containing candidate nodes for the right and left hyperedges, and  $x = \lambda_{\tilde{h}_{n+1,m}}(t)$  is parameterized by a neural network  $f(\cdot)$  that take embedding of nodes in  $h_{n+1,m}$  at time  $t$  as input as shown below,

$$\lambda_{h_{n+1,m}}(t) = f(\{\mathbf{v}_i(t)\}_{v_i \in h_{n+1,m}^r}, \{\mathbf{v}_i(t)\}_{v_i \in h_{n+1,m}^l}).$$

The architecture of  $f(\cdot)$  is explained in Section 4.

#### 3.4 Loss Function

The likelihood for forecasting  $(e_{n+1}, t_{n+1})$  given the past interaction  $\mathcal{E}(t_n)$  is the product of time and hyperedge prediction likelihoods in Equations 1 and 3,

$$p((e_{n+1}, t_{n+1})|\mathcal{E}(t_n)) = p((\cup e_{n+1}, t_{n+1})|\mathcal{E}(t_n)) p(\mathcal{H}_{n+1}, \mathcal{Y}_{n+1}|\cup e_{n+1}, t_{n+1}, \mathcal{E}(t_n)). \quad (4)$$

The complete likelihood is as follows,

$$p(\mathcal{E}(t_N)) = \prod_{n=0}^{N-1} p((e_{n+1}, t_{n+1}) | \mathcal{E}(t_n)). \quad (5)$$

For training the parameters of the model, we minimize the following negative loglikelihood as follows,

$$\begin{aligned} \mathcal{L} &= -1 \sum_{n=0}^{N-1} \log p((e_{n+1}, t_{n+1}) | \mathcal{E}(t_n)) \\ &= -1 \sum_{n=0}^{N-1} (\log p((\cup e_{n+1}, t_{n+1}) | \mathcal{E}(t_n)) \\ &\quad + \log p(\mathcal{H}_{n+1}, \mathcal{Y}_{n+1} | \cup e_{n+1}, t_{n+1}, \mathcal{E}(t_n))). \end{aligned} \quad (6)$$

Then substituting their respective values, we can express the loss as follows,

$$\begin{aligned} \mathcal{L} &= -1 \sum_{n=0}^{N-1} \left[ \sum_{v_i \in \cup e_{n+1}^r} \log(\mu_{n+1,i}^r) + \sum_{v_i \in \mathcal{V}} -\mu_{n+1,i}^r (t_{n+1} - t_n) \right] \\ &\quad -1 \sum_{n=0}^{N-1} \left[ \sum_{v_i \in \cup e_{n+1}^l} \log(\mu_{n+1,i}^l) + \sum_{v_i \in \mathcal{V}} -\mu_{n+1,i}^l (t_{n+1} - t_n) \right] \\ &\quad - \sum_{n=0}^{N-1} \left[ \sum_{\tilde{h}_{n+1,j} \in \tilde{\mathcal{H}}_{n+1}} [y_{\tilde{h}_{n+1,j}} \log \lambda_{\tilde{h}_{n+1,j}}(t) \right. \\ &\quad \left. + (1 - y_{\tilde{h}_{n+1,j}}) \log(1 - \lambda_{\tilde{h}_{n+1,j}}(t))] \right]. \end{aligned}$$

While training the candidate negative hyperedges with  $y_{\tilde{h}_{n+1,m}} = 0$  are generated by corrupting either left or right hyperedge with a hyperedge of randomly sampled size and filled with random nodes.

## 4 Architecture of Hyperedge Predictor

Previous approaches to predict hyperedges involve HyperSAGNN [Zhang *et al.*, 2020] for undirected hyperedge, and CATSETMAT [Sharma *et al.*, 2021] for bipartite hyperedge. As explained in earlier the section, they cannot fully model the three types of relations shown by a directed hyperedge. That involves two homogeneous interactions in the right and left hyperedges, and the cross interaction across the left and right hyperedge. Here, we propose an architecture that utilizes all three interactions to predict true hyperedge from fake ones. Given a directed hyperedge  $h = (\{v_1, \dots, v_k\}, \{v_{1'}, \dots, v_{k'}\})$ , we use the cross-attention layer, *CAT*, between the sets of nodes to create dynamic embeddings as shown below,

$$\begin{aligned} \mathbf{d}_i^{ch} &= \text{CAT}(\{v_1(t), \dots, v_k(t)\}, \{v_{1'}(t), \dots, v_{k'}(t)\}) \\ \mathbf{d}_i^{c'h} &= \text{CAT}(\{v_{1'}(t), \dots, v_{k'}(t)\}, \{v_1(t), \dots, v_k(t)\}) \end{aligned} \quad (7)$$

These dynamic hyperedge embeddings are then added to the original embeddings to get embeddings,  $\mathbf{z}_i(t) = \mathbf{v}_i(t) + \mathbf{d}_i^{ch}$ , then we pass these through a self-attention layer, *SAT*,

$$\begin{aligned} \mathbf{d}_i^{ch} &= \text{SAT}(\{v_1(t), \dots, v_k(t)\}) \\ \mathbf{d}_i^{c'h} &= \text{SAT}(\{v_{1'}(t), \dots, v_{k'}(t)\}) \end{aligned} \quad (8)$$

The dynamic hyperedge embeddings from Equations 7 and 8 are combined to get the complete dynamic hyperedge embeddings,  $\mathbf{d}_i^h = \mathbf{d}_i^{sh} + \mathbf{d}_i^{ch}$ . We also create static hyperedge embeddings  $\mathbf{s}_i^h = \mathbf{W}_s \mathbf{v}_i(t)$ , where  $\mathbf{W}_s \in \mathbb{R}^{d \times d}$  is a learnable parameter. Then we calculate the Hadamard power of the difference between static and dynamic hyperedge embedding pairs followed by a linear layer and average pooling to get the final score  $\mathcal{P}^h$  as shown below,

$$\begin{aligned} o_i &= \mathbf{W}_o^T [(\mathbf{d}_i^h - \mathbf{v}_i(t))^2; (\mathbf{d}_i^{ch} - \mathbf{s}_i^h)^2] + b_o, \\ \mathcal{P}^{hr} &= \frac{1}{k} \sum_{i=1}^k \mathcal{P}_i^h = \frac{1}{k} \sum_{i=1}^k \log(1 + \exp(o_i)). \end{aligned} \quad (9)$$

Here,  $\mathbf{W}_o \in \mathbb{R}^{2d \times 1}$ ,  $b_o \in \mathbb{R}$  are learnable parameters of the output layer. Similarly, we find  $\mathcal{P}^{hl}$  for the left hyperedge with a different set of parameters, and we combine them to predict links. So, in our model the value of  $f(\{v_1(t), v_2(t), \dots, v_k(t)\} \{v_{1'}(t), v_{2'}(t), \dots, v_{k'}(t)\}) = \mathcal{P}^{hr} + \mathcal{P}^{hl}$ . The model's entire block architecture and details of *CAT* and *SAT* are shown in Appendix B.

## 5 Dynamic Node Embedding

The dynamic embedding of node  $v_i$  have the following architecture,

$$\mathbf{v}_i(t) = \tanh(\mathbf{W}^s \text{Mem}_{v_i} + \mathbf{W}^r \mathbf{v}_i^r(t) + \mathbf{W}^l \mathbf{v}_i^l(t) + \mathbf{b}_0). \quad (10)$$

Here,  $\mathbf{W}^s \in \mathbb{R}^{d \times d}$ ,  $\mathbf{W}^r \in \mathbb{R}^{d \times d}$ ,  $\mathbf{W}^l \in \mathbb{R}^{d \times d}$  and  $\mathbf{b}_0 \in \mathbb{R}^d$  are learnable parameters. The first term,  $\text{Mem}_{v_i} \in \mathbb{R}^d$  is the historical interaction information for node  $v_i$  stored in the Memory Module explained in Section 5.1. In the second term,  $\mathbf{v}_i^r(t)$  is the Temporal embeddings calculated based on the recent higher-order interactions  $h$  where the node  $v_i$  is present in the right hyperedge,  $h^r \cap \{v_i\} \neq \emptyset$ . Similarly, we calculate  $\mathbf{v}_i^l(t)$  based on the interactions where a node is present in the left hyperedge. The architecture used for finding these embeddings are shown in Section 5.2.

### 5.1 Memory Module

The entities in a network evolve with each interaction and show temporal trends in their interaction pattern. To efficiently capture these, we learn a dynamic representation for each node in the network, which is a function of time and historical interactions. In our work, Memory module  $\text{Mem} \in \mathbb{R}^{|\mathcal{V}| \times d}$  stores the historical interaction information for each node in the network till time  $t$ . This module is initialized with random features, and when a node is involved in an interaction, its corresponding features are updated based on the output of the Message Generation Module. However, if we update the node embeddings with each interaction like in the previous works [Gracious and Dukkupati, 2023], we will not be able to scale the model to a large number of samples. So, we divide the interactions into batches of size  $b$

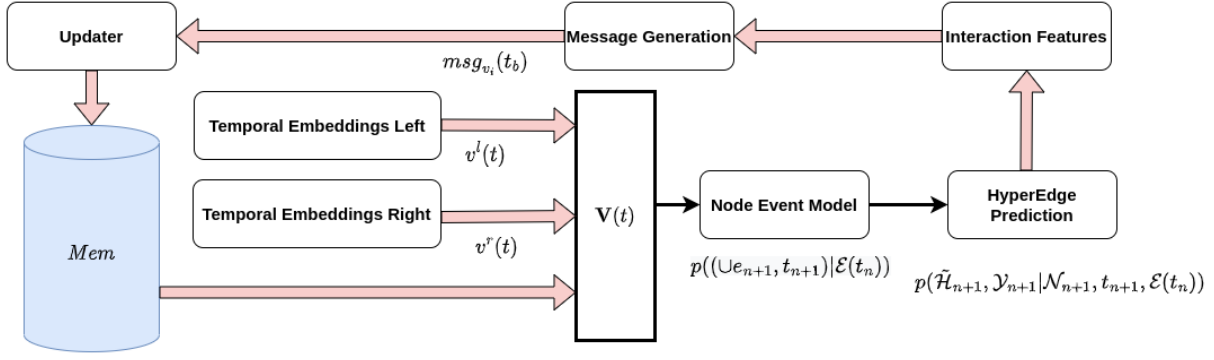


Figure 2: Neural Architecture of DHyperNodeTPP: We calculate the dynamic node embeddings  $\mathbf{V}(t)$  by combining the embeddings from the Memory module with information from recent interactions where the node was involved in the left and right hyperedges. These dynamic embeddings are used to forecast nodes in which events are occurring. Then the hyperlink prediction decoder is shown in Section 4 is used to find the observed hyperedges.

while maintaining their temporal order. Then we aggregate the temporal features of each node in the batch using the Message Generation stage 5.1. Then we update the memory embeddings of the node using a recurrent neural network as explained in Memory Update stage 5.1.

### Message Generation

We calculate features for each node in all interactions in a batch  $(h_i, t_i)_{i=1}^b$ . For node  $v_i$  in the right hyperedge  $h_i^r$  of interaction  $h_i$  at time  $t_i$ , the features are the concatenation of its dynamic embedding  $v_i(t)$ , dynamic hyperedge embeddings  $\mathbf{d}_i^h$ , Fourier features [da Xu *et al.*, 2020] calculated from the duration  $t - t_{v_i}^p$  since the last memory update of that node happened at time  $t_{v_i}^p$ , and positional feature. This can be shown as

$$\text{msg}_{v_i}(t_i) = [v_i(t); \mathbf{d}_i^h; \Phi(t - t_{v_i}^p); \text{side}]. \quad (11)$$

Here,  $\text{side}$  is the positional feature with a value 1 for right hyperedge, and  $\Phi(t - t_{v_i}^p) \in \mathbb{R}^d$  is the Fourier features [da Xu *et al.*, 2020] based on functional encoding for the time  $t - t_{v_i}^p$ . This is achieved by learning a mapping function  $\Phi(t) = [\cos(\omega_1 t + \theta_1), \dots, \cos(\omega_d t + \theta_d)]$  with parameters  $\{\omega_i\}_{i=1}^d$ , and  $\{\theta_i\}_{i=1}^d$  inferred from the data. Similarly, we will calculate the interaction features ( $\text{msg}(\cdot)$ ) for nodes in the left hyperedge with  $\text{side} = -1$ .

### Memory Update

The messages from the previous section are used to update the Memory Module  $Mem$  entries of the corresponding nodes before the next batch. In our work, we use a GRU [Cho *et al.*, 2014] based recurrent neural networks for memory updating as shown below,

$$Mem_{v_i} = \text{Updater}(\text{msg}_{v_i}(t_b), Mem_{v_i}(t_{v_i}^p)). \quad (12)$$

Then,  $t_{v_i}^p$  is updates to latest interaction time where  $v_i$  is present in the batch,  $t_{v_i}^p = \max_{v_i \in h_i, 0 \leq i \leq b} t_i$ .

## 5.2 Temporal Embeddings

To incorporate higher-order neighborhood information into the node embeddings, we use a temporal graph attention network to update the node representation with information from

relevant historical interactions. Further, it also helps avoid the staleness [Kazemi *et al.*, 2020] of embeddings in the Memory Module due to the absence of recent interactions involving the node by extracting information from other nodes that are previously involved with it.

For a node  $v_i$  at time  $t$ , we find the recent  $N$  interactions involving the node in the right hyperedge, and we denote them as,  $\mathcal{N}_{h^r}(t)$ . Then for each hyperedge  $(h_i, t_i) \in \mathcal{N}_{h^r}(t)$ , we calculate the hyperedge features as shown below,

$$h^r(t_i) = \frac{1}{|h^r|} \sum_{v_i \in h^r} \mathbf{W}_h^r Mem_{v_i} + \frac{1}{|h^l|} \sum_{v_i \in h^l} \mathbf{W}_h^l Mem_{v_i}. \quad (13)$$

Similarly, we find the recent  $N$  interactions where nodes are in the left hyperedge,  $\mathcal{N}_{h^l}(t)$ , and calculate hyperedge embeddings  $h^l(t_i)$  using Equation 13. Then we the right hyperedge embeddings using the temporal graph attention layer shown below,

$$\begin{aligned} v^r(t) &= \text{MultiHeadAttention}(\mathbf{q}(t), \mathbf{K}(t), \mathbf{V}(t)) \\ \mathbf{Q}(t) &= Mem_v || \phi(0) \\ \mathbf{K}(t) &= \mathbf{V}(t) \\ \mathbf{V}(t) &= [h^r(t_1) || \phi(t - t_1), \dots, h^r(t_N) || \phi(t - t_N)]. \end{aligned} \quad (14)$$

Here,  $||$  is the concatenation operator. The multi-head-attention layer [Vaswani *et al.*, 2017] uses the node embeddings for query ( $\mathbf{Q}(t)$ ), and recent interaction embeddings as keys ( $\mathbf{K}(t)$ ) and values ( $\mathbf{V}(t)$ ). Similarly, we calculate  $v^l(t)$  using a separate multi-head-attention layer.

## 6 Prediction Tasks

We create two tasks to evaluate our model’s event forecasting capabilities and to compare its performance against baseline methods.

**Interaction Type Prediction.** The goal of this task is to predict the type of interaction  $e_{n+1}$  occurring at time  $t_{n+1}$  given the past interaction  $\mathcal{E}(t_n)$ . It can be done using Equation 3 with candidate hyperedges  $\mathcal{H}_{n+1}^c$  generated using Equation 2.

Datasets	$ \mathcal{V} $	$ \mathcal{E}(T) $	$ \mathcal{H}^r $	$ \mathcal{H}^l $	$T$
Enron-Email	183	10,311	1,003	89	99,070.18
Twitter	2,130	9,889	1,218	2,321	17,277.80
HepTh	451	9,882	8,384	1,352	21,532.70
ML-ArXiv	659	18,558	2,995	17,014	62,741.56
iAF1260b	1,668	2,084	2,010	1,985	N/A
iJO1366	1,805	2,253	2,174	2,146	N/A
USPTO	16,293	11,433	6,819	6,784	N/A

Table 1: Datasets used for Temporal and Static Directed Hypergraphs along with their vital statistics.

**Interaction Time Prediction.** The goal of this task is to predict the next time of interaction  $t_{n+1}$  given the past interaction  $\mathcal{E}(t_n)$  for the nodes of interest  $\cup e_{n+1}$ . It can be calculated using the time estimate  $\hat{t}_{n+1,i} = \frac{1}{\mu_{n+1,i}}$  for each node  $v_i \in \cup e_{n+1}$ .

## 7 Datasets

Table 1 shows the statistics of the both static and temporal directed datasets. Here,  $|\mathcal{V}|$  denotes the number of nodes,  $|\mathcal{E}(T)|$  denotes the number of hyperedges,  $|\mathcal{H}^r|$  denotes the number of unique right hyperedges,  $|\mathcal{H}^l|$  denotes the number of unique left hyperedges, and  $T$  is the time span of the dataset. For the static datasets there is no time span feature. A more detailed description of each dataset is provided in Appendix C.

## 8 Experiments

### 8.1 Baseline Models

**HyperNodeTPP.** This is an undirected version of our model DHyperNodeTPP with right and left hyperedge merged into a single hyperedge,  $h = h^r \cup h^l$ . This uses the same Dynamic embedding in Section 5 with only a single type of Temporal Embeddings 5.2 and the HyperSANN [Zhang *et al.*, 2020] architecture for hyperedge prediction. The node event modeling in Section 3.2 is done by considering only a single type of node event.

**HGBDHE, HGDHE.** These models are taken from previous work [Gracious and Dukkipati, 2023] for higher-order interaction forecasting. They use hyperedge level events to model higher-order interactions and use a recurrent model to learn dynamic node embedding by updating them when an interaction occurring. Here, **HGDHE** is developed for undirected hyperedge event forecasting, and **HGBDHE** is developed for bipartite hyperedge forecasting.

**TGN, GAT.** These are pairwise models developed for forecasting pairwise interaction. Here, **TGN**[Rossi *et al.*, 2020] is developed for forecasting events in a dynamic graph. **GAT** [Veličković *et al.*, 2018] is a static model that predict presence or absence of a link in a static graph.

Appendix D contains a more detailed description of each baseline.

## 8.2 Metrics of Evaluations

**Mean Average Reciprocal Rank (MRR)** For evaluating the performance of interaction type prediction at time  $t$ , we find the position of true hyperedges  $r_n$  against candidate negative hyperedges by ordering them in descending order of  $\lambda_h(t)$  of. Here, negative hyperedges are calculated by removing the entire left or right hyperedges by randomly sampled nodes. Then MRR is calculated as follows,

$$MRR = \frac{1}{N} \sum_{n=1}^N \frac{1}{r_n + 1}. \quad (15)$$

**Mean Average Error (MAE)** For evaluating the performance of interaction time at time  $t$ , we find the average of absolute difference between true values  $t^{true}$  and estimated value  $\hat{t}_{n+1,i}$  as shown below,

$$MAE = \frac{1}{2N} \sum_{n=1}^N \left[ \sum_{v_i \in \cup e_n^r} \frac{1}{|\cup e_n^r|} |t_n^{true} - \hat{t}_{n,i}| + \sum_{v_i \in \cup e_n^l} \frac{1}{|\cup e_n^l|} |t_n^{true} - \hat{t}_{n,i}| \right]. \quad (16)$$

## 8.3 Settings

In all our experiments, we use the first 50% of hyperedges for training, 25% for validation, and the remaining 25% for testing. We used the Adam optimizer and the ExponentialLR scheduler with  $\gamma = 0.95$  to train the models for 100 epochs with the batch size set to 128 and a learning rate of 0.001. Models have a fixed embedding size  $d$  of 64, and we use 20 negative hyperedges for each true hyperedge in the dataset. All the reported scores are the average of ten randomized runs, along with their standard deviation.

## 8.4 Results

Our proposed model DHyperNodeTPP is evaluated against previous works and an undirected baseline model, HyperNodeTPP. The results in Table 2 demonstrate that our models, HyperNodeTPP and DHyperNodeTPP, outperformed previous works, HGDHE and HGBDHE, in interaction time prediction. This superior performance can be attributed to the fact that our models are trained to predict the next event on the nodes, as opposed to previous models, which were trained to predict the next event on a hyperedge. Their task is more difficult and prone to error as they have to predict events of longer duration. However, in our case, events on nodes are more frequent and of shorter periods, hence the lesser error in the time duration prediction. Further, one can observe that the dynamic models perform much better than the static model GAT [Veličković *et al.*, 2018]. This shows the need for dynamic models for real-world interaction forecasting. In our work, we achieve this using a Memory based dynamic node representation learning technique as explained in Section 5. We can also observe that models that use attention-based dynamic embeddings, HyperNodeTPP and DHyperNodeTPP, performs better than non-attentional models, HGBDHE and HGDHE, by comparing the performance in interaction-type prediction task. This justifies the use of Temporal Embedding in Section 5.2 for dynamic node representation learning.

Methods		GAT	TGN	HGDHE	HGBDHE	HyperNodeTPP(ours)	DHyperNodeTPP(ours)
<b>Enron-Email</b>	MAE	<i>N/A</i>	<i>N/A</i>	35.77 ± 1.61	13.92 ± 0.35	<b>4.15 ± 0.01</b>	4.17 ± 0.01
	MRR	40.16 ± 7.15	42.22 ± 0.87	35.00 ± 3.94	36.09 ± 1.96	62.75 ± 2.26	<b>63.94 ± 1.80</b>
<b>Twitter</b>	MAE	<i>N/A</i>	<i>N/A</i>	21.58 ± 3.79	8.16 ± 0.70	1.35 ± 0.02	<b>1.29 ± 0.009</b>
	MRR	44.88 ± 0.05	55.20 ± 0.03	69.87 ± 0.72	70.19 ± 0.95	77.00 ± 0.75	<b>79.32 ± 0.36</b>
<b>HepTh</b>	MAE	<i>N/A</i>	<i>N/A</i>	16.19 ± 3.01	8.86 ± 0.08	4.89 ± 0.39	<b>1.27 ± 0.04</b>
	MRR	33.79 ± 8.95	51.70 ± 1.37	<b>57.98 ± 0.82</b>	57.40 ± 3.00	52.02 ± 0.57	55.57 ± 1.28
<b>ML-ArXiv</b>	MAE	<i>N/A</i>	<i>N/A</i>	29.94 ± 3.77	17.29 ± 0.57	<b>0.99 ± 0.04</b>	<b>0.99 ± 0.04</b>
	MRR	22.49 ± 4.31	37.58 ± 1.12	26.07 ± 0.29	28.13 ± 0.78	26.04 ± 0.09	<b>37.72 ± 0.84</b>

Table 2: Performance of dynamic directed hyperedge forecasting in tasks of interaction type and interaction duration prediction. The proposed model DHyperNodeTPP beats baseline models in almost all the time prediction tasks. Here, interaction type prediction is evaluated using MRR %; here higher value indicates better performance, and interaction duration prediction is evaluated using MAE, lower value indicates better performance.

**Comparing directed and undirected models.** The advantage of directed modeling can be observed by comparing the performance of directed models to their undirected equivalents. For example, when comparing the directed model DHyperNodeTPP with HyperNodeTPP, we see an average increase of 14% in the MRR metric for interaction type prediction. Similar improvements can be observed when comparing the performance of previous works, HGBDHE and HGDHE. As the bipartite model HGBDHE incorporates directionality information, there is an average improvement of 2% in the MRR metric for interaction type prediction. Additionally, the MAE metric for interaction time prediction is reduced by 53% when using the HGBDHE model compared to the HGDHE model. Hence, incorporating directionality information improves the forecasting ability of the models.

**Comparing hyperedge models with the pairwise model.** The advantage of hyperedge models over pairwise edge models can be inferred by comparing models DHyperNodeTPP to TGN, which is the pairwise equivalent of DHyperNodeTPP. Our model DHyperNodeTPP has an average improvement of 34.8% in MRR metric over TGN in interaction type prediction. Similarly, HGBDHE model performs better than TGN for Twitter and Hepth datasets as it uses hyperedge models for interaction type prediction.

Methods	HyperSAGNN	CATSETMAT	Ours
<b>iAF1260b</b>	<b>60.14 ± 2.49</b>	35.08 ± 1.4	58.48 ± 1.47
<b>iJO1366</b>	57.94 ± 1.82	36.22 ± 0.95	<b>59.07 ± 1.78</b>
<b>USPTO</b>	35.94 ± 1.87	37.84 ± 0.58	<b>38.59 ± 0.41</b>

Table 3: Performance of our hyperedge predictor in Section 4 to previous works Hyper-SAGNN and CATSETMAT on static directed hyperedge prediction. Here, the MRR metric is used to evaluate the performance.

**Comparing different hyperedge prediction architecture.** In Table 3, we compared our directed hyperedge predictor to previous works, HyperSANN [Zhang *et al.*, 2020] for undirected hyperlink prediction, and CATSETMAT [Sharma *et al.*, 2021] for bipartite hyperlink prediction. Our method performs considerably better than previous architectures. We are

getting an average improvement of 2% over the undirected model and 43% over the bipartite model in MRR metric. This is because our link predictor models self-connections in both right and left hyperedges and also cross edges between them. The poor performance of CATSETMAT is because it focuses on modeling the cross connections and fails to model self connections in both right and left hyperedge due to the bipartite assumption.

## 9 Conclusion

In this work, we present the model **DHyperNodeTPP** to forecast higher-order directed interactions based on historical data. Most of the previous works [da Xu *et al.*, 2020; Trivedi *et al.*, 2019; Gracious *et al.*, 2021; Kumar *et al.*, 2019] either reduce higher-order interactions as pairwise interactions or ignore the directionality [Gracious and Dukkipati, 2023] information in the interactions. Further, previous work [Gracious and Dukkipati, 2023] in hyperedge forecasting also suffers from scalability issues while forecasting future interaction. They model them as a marked temporal point process with each hyperedge as a separate mark, and the number of unique hyperedges is exponential to the number of nodes. So, to address this, we use a multi-task approach involving two stages. The first stage is used to forecast nodes where the events will occur that are then consumed by the second task, which uses a directed hyperlink prediction module. Since the number of nodes that observe an event at a particular time is tiny, we could considerably reduce the search space for the possible hyperedge. Further, we provide a dynamic representation learning framework that can do batch training by using a Memory Module. This reduces computational complexity while training on datasets with large number of interactions. We also provided an architecture for directed hyperedge prediction by combining three levels of relationship in it. We created four datasets to show the advantage of our model over existing models for undirected and bipartite hyperedge forecasting models. In future work, we want to explore advanced negative sampling techniques [Hwang *et al.*, 2022] to make the model learn efficiently and provide good candidate hyperedges in a scalable way. Further, we also like to explore the possibility of incorporating multi-hop information in a scalable way for dynamic representation learning.

## References

- [Bai *et al.*, 2021] Song Bai, Feihu Zhang, and Philip HS Torr. Hypergraph convolution and hypergraph attention. *Pattern Recognition*, 110:107637, 2021.
- [Benson *et al.*, 2018] Austin R. Benson, Rediet Abebe, Michael T. Schaub, Ali Jadbabaie, and Jon Kleinberg. Simplicial closure and higher-order link prediction. *Proceedings of the National Academy of Sciences*, 115(48):E11221–E11230, 2018.
- [Cao *et al.*, 2021] Jiangxia Cao, Xixun Lin, Xin Cong, Shu Guo, Hengzhu Tang, Tingwen Liu, and Bin Wang. Deep structural point process for learning temporal interaction networks. In *Joint European Conference on Machine Learning and Knowledge Discovery in Databases*, pages 305–320. Springer, 2021.
- [Cho *et al.*, 2014] Kyunghyun Cho, Bart van Merriënboer, Caglar Gulcehre, Dzmitry Bahdanau, Fethi Bougares, Holger Schwenk, and Yoshua Bengio. Learning phrase representations using RNN encoder–decoder for statistical machine translation. In *Proceedings of the 2014 Conference on Empirical Methods in Natural Language Processing (EMNLP)*, pages 1724–1734. Association for Computational Linguistics, October 2014.
- [Chodrow and Mellor, 2019] Philip Chodrow and Andrew Mellor. Annotated hypergraphs: Models and applications, 2019.
- [da Xu *et al.*, 2020] da Xu, chuanwei ruan, evren korpeoglu, sushant kumar, and kannan achan. Inductive representation learning on temporal graphs. In *International Conference on Learning Representations*, 2020.
- [Feng *et al.*, 2019] Yifan Feng, Haoxuan You, Zizhao Zhang, Rongrong Ji, and Yue Gao. Hypergraph neural networks. In *Proceedings of the AAAI conference on artificial intelligence*, pages 3558–3565, 2019.
- [Gehrke *et al.*, 2003] Johannes Gehrke, Paul Ginsparg, and Jon Kleinberg. Overview of the 2003 kdd cup. *SIGKDD Explor. Newsl.*, 5(2):149–151, dec 2003.
- [Ghoshdastidar and Dukkipati, 2017] Debarghya Ghoshdastidar and Ambedkar Dukkipati. Consistency of spectral hypergraph partitioning under planted partition model. *The Annals of Statistics*, 45(1):289 – 315, 2017.
- [Gracious and Dukkipati, 2023] Tony Gracious and Ambedkar Dukkipati. Dynamic representation learning with temporal point processes for higher-order interaction forecasting. In *AAAI*, 2023.
- [Gracious *et al.*, 2021] Tony Gracious, Shubham Gupta, Arun Kanthali, Rui M Castro, and Ambedkar Dukkipati. Neural latent space model for dynamic networks and temporal knowledge graphs. In *Proceedings of the AAAI Conference on Artificial Intelligence*, volume 35, pages 4054–4062, 2021.
- [Hawkes, 1971] Alan G. Hawkes. Spectra of some self-exciting and mutually exciting point processes. *Biometrika*, 58(1):83–90, 1971.
- [Hwang *et al.*, 2022] Hyunjin Hwang, Seungwoo Lee, Chanyoung Park, and Kijung Shin. Ahp: Learning to negative sample for hyperedge prediction. In *Proceedings of the 45th International ACM SIGIR Conference on Research and Development in Information Retrieval, SIGIR '22*, page 2237–2242, New York, NY, USA, 2022. Association for Computing Machinery.
- [Kazemi *et al.*, 2020] Seyed Mehran Kazemi, Rishab Goel, Kshitij Jain, Ivan Kobyzev, Akshay Sethi, Peter Forsyth, and Pascal Poupart. Representation learning for dynamic graphs: A survey. *J. Mach. Learn. Res.*, 21(70):1–73, 2020.
- [Kim *et al.*, 2022] Sunwoo Kim, Minyoung Choe, Jaemin Yoo, and Kijung Shin. Reciprocity in directed hypergraphs: Measures, findings, and generators. In *ICDM*, 2022.
- [Kumar *et al.*, 2019] Srijan Kumar, Xikun Zhang, and Jure Leskovec. Predicting dynamic embedding trajectory in temporal interaction networks. In *Proceedings of the 25th ACM SIGKDD international conference on Knowledge discovery and data mining*. ACM, 2019.
- [Liu *et al.*, 2018] Zheng Liu, Xing Xie, and Lei Chen. Context-aware academic collaborator recommendation. In *Proceedings of the 24th ACM SIGKDD International Conference on Knowledge Discovery & Data Mining*, pages 1870–1879, 2018.
- [Liu *et al.*, 2022] Yunyu Liu, Jianzhu Ma, and Pan Li. Neural predicting higher-order patterns in temporal networks. In *Proceedings of the ACM Web Conference 2022*, pages 1340–1351, 2022.
- [Lowe, ] D. M. Lowe. Patent reaction extraction , download : <https://github.com/dan2097/patent-reaction-extraction>.
- [Mei and Eisner, 2017] Hongyuan Mei and Jason M Eisner. The neural hawkes process: A neurally self-modulating multivariate point process. In *Advances in Neural Information Processing Systems*, volume 30. Curran Associates, Inc., 2017.
- [Ng and Murphy, 2021] Tin Lok James Ng and Thomas Brendan Murphy. Model-based clustering for random hypergraphs. *Advances in Data Analysis and Classification*, pages 1–33, 2021.
- [Ranshous *et al.*, 2017] Stephen Ranshous, Cliff A. Joslyn, Sean Kreyling, Kathleen Nowak, Nagiza F. Samatova, Curtis L. West, and Samuel Winters. Exchange pattern mining in the bitcoin transaction directed hypergraph. In Michael Brenner, Kurt Rohloff, Joseph Bonneau, Andrew Miller, Peter Y.A. Ryan, Vanessa Teague, Andrea Bracciali, Massimiliano Sala, Federico Pintore, and Markus Jakobsson, editors, *Financial Cryptography and Data Security*, pages 248–263, Cham, 2017. Springer International Publishing.
- [Rossi *et al.*, 2020] Emanuele Rossi, Ben Chamberlain, Fabrizio Frasca, Davide Eynard, Federico Monti, and Michael Bronstein. Temporal graph networks for deep learning on dynamic graphs. In *ICML 2020 Workshop on Graph Representation Learning*, 2020.

- [Sankar *et al.*, 2020] Aravind Sankar, Yanhong Wu, Liang Gou, Wei Zhang, and Hao Yang. Dysat: Deep neural representation learning on dynamic graphs via self-attention networks. In *Proceedings of the 13th international conference on web search and data mining*, pages 519–527, 2020.
- [Sharma *et al.*, 2021] Govind Sharma, Swyam Prakash Singh, V Susheela Devi, and M Narasimha Murty. The cat set on the mat: Cross attention for set matching in bipartite hypergraphs, 2021.
- [Stasi *et al.*, 2014] Despina Stasi, Kayvan Sadeghi, Alessandro Rinaldo, Sonja Petrovic, and Stephen E Fienberg.  $\beta$  models for random hypergraphs with a given degree sequence. In *International Conference on Computational Statistics*, 2014.
- [Trivedi *et al.*, 2019] Rakshit Trivedi, Mehrdad Farajtabar, Prasenjeet Biswal, and Hongyuan Zha. Dyrep: Learning representations over dynamic graphs. In *International conference on learning representations*, 2019.
- [Vaswani *et al.*, 2017] Ashish Vaswani, Noam Shazeer, Niki Parmar, Jakob Uszkoreit, Llion Jones, Aidan N Gomez, Łukasz Kaiser, and Illia Polosukhin. Attention is all you need. In I. Guyon, U. Von Luxburg, S. Bengio, H. Wallach, R. Fergus, S. Vishwanathan, and R. Garnett, editors, *Advances in Neural Information Processing Systems*, volume 30. Curran Associates, Inc., 2017.
- [Veličković *et al.*, 2018] Petar Veličković, Guillem Cucurull, Arantxa Casanova, Adriana Romero, Pietro Liò, and Yoshua Bengio. Graph attention networks. In *International Conference on Learning Representations*, 2018.
- [Yadati *et al.*, 2019] Naganand Yadati, Madhav Nimishakavi, Prateek Yadav, Vikram Nitin, Anand Louis, and Partha Talukdar. Hypergcn: A new method for training graph convolutional networks on hypergraphs. In *Advances in Neural Information Processing Systems*, volume 32, 2019.
- [Yadati *et al.*, 2020] Naganand Yadati, Vikram Nitin, Madhav Nimishakavi, Prateek Yadav, Anand Louis, and Partha Talukdar. Nhp: Neural hypergraph link prediction. In *Proceedings of the 29th ACM International Conference on Information & Knowledge Management*, pages 1705–1714, 2020.
- [Zhang *et al.*, 2018] Muhan Zhang, Zhicheng Cui, Shali Jiang, and Yixin Chen. Beyond link prediction: Predicting hyperlinks in adjacency space. In *AAAI*, 2018.
- [Zhang *et al.*, 2020] Ruochi Zhang, Yuesong Zou, and Jian Ma. Hyper-sagnn: a self-attention based graph neural network for hypergraphs. In *International Conference on Learning Representations*, 2020.
- [Zhou *et al.*, 2006] Dengyong Zhou, Jiayuan Huang, and Bernhard Schölkopf. Learning with hypergraphs: Clustering, classification, and embedding. In B. Schölkopf, J. Platt, and T. Hoffman, editors, *Advances in Neural Information Processing Systems*, volume 19, 2006.

# Neural Temporal Point Process for Forecasting Higher Order and Directional Interactions: Appendix

## A Background on Temporal Point Process

A temporal point process (TPP) defines a probability distribution over discrete events happening in continuous time. It can be shown as a sequence of timestamps  $\mathcal{E}(t_n) = \{t_0, t_1, \dots, t_n\}$ , here  $t_n$  is the time of occurrence of the event. The goal of temporal point process is to model the probability of next event given the history  $p(t_{n+1}|t_0, \dots, t_n)$ . A marked temporal point process is a type of TPP, where each event is associated with a category  $c \in \mathcal{C}$ . Here,  $\mathcal{C}$  can be a set of discrete objects or a feature vector of real values. This can be represented as  $\mathcal{E}(t_n) = \{(t_0, c_0), (t_1, c_1), \dots, (t_n, c_n)\}$ . A temporal point process can be parameterized by an intensity function  $\lambda(t)$ ,

$$\lambda(t)dt = p(\text{event in } [t, t + dt] \mid \mathcal{E}(t_n)). \quad (17)$$

Then the likelihood of the next event time can be modeled as

$$p(t|\mathcal{E}(t_n)) = \lambda(t)\mathcal{S}(t),$$

$$\mathcal{S}(t) = \exp\left(\int_{t_n}^t -\lambda(\tau)d\tau\right). \quad (18)$$

Here,  $\mathcal{S}(t)$  is called the survival function representing the probability of the event not occurring during the interval  $[t_n, t)$ . The likelihood for the entire observation  $\mathcal{E}(T)$  in the duration  $[0, T]$  can be written as follows,

$$p(\mathcal{E}(T)) = \prod_{n=0}^{|\mathcal{E}(T)|} \lambda(t_n)\mathcal{S}(T). \quad (19)$$

Here,  $\mathcal{S}(T) = \prod_{n=0}^{|\mathcal{E}(T)|} \mathcal{S}(t_n) = \exp\left(\int_0^T -\lambda(\tau)d\tau\right)$ .

The popular function forms of a temporal point process are exponential distribution  $\lambda(t) = \mu$ , where  $\mu > 0$  is the rate of event. Hawkes process [Hawkes, 1971] is another widely used method when events have self exciting nature with  $\lambda(t) = \mu + \alpha \sum_{t_n \in \mathcal{E}(t)} \mathcal{K}(t - t_n)$ . Here,  $\mu \geq 0$  is the base rate,  $\mathcal{K}(t) \geq 0$  is the excitation kernel, and  $\alpha \geq 0$  is the strength of excitation. If  $\lambda(t) = f(\mathcal{E}(t))$  with  $f(\cdot)$  as a neural network, then it is called a neural temporal point process [Mei and Eisner, 2017].

## B Hyperedge Predictor Architecture Details

Figure 3 shows the block diagram of the directed hyperedge predictor used in our model DHyperNodeTPP. The following are the attention layers used in our model.

**CAT.** Given a directed hyperedge  $h = (\{v_1, \dots, v_k\}, \{v_{1'}, \dots, v_{k'}\})$ , we use the cross-attention layer between the sets of nodes to create dynamic embed-

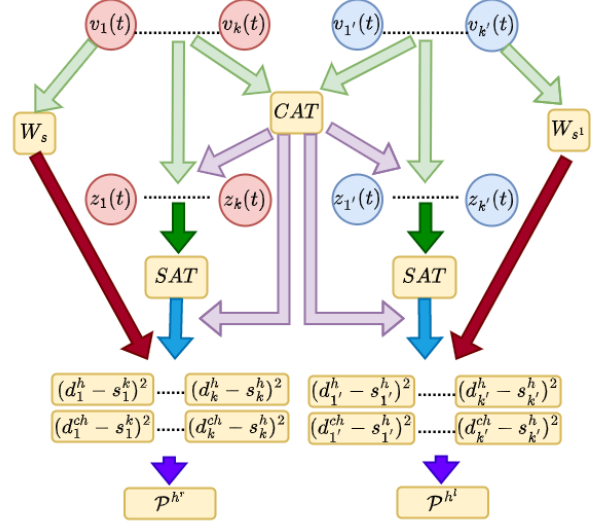


Figure 3: Hyperedge Predictor Architecture

dings as shown below,

$$e_{ij'} = (\mathbf{W}_{CQ}^T \mathbf{v}_i(t)) \mathbf{W}_{CK'}^T \mathbf{v}_{j'}(t), 1 \leq i \leq k, 1 \leq j' \leq k',$$

$$e_{i'j} = (\mathbf{W}_{CQ'}^T \mathbf{v}_{i'}(t)) \mathbf{W}_{CK}^T \mathbf{v}_j(t), 1 \leq i' \leq k', 1 \leq j \leq k$$

$$\alpha_{ij'} = \frac{\exp(e_{ij'})}{\sum_{1 \leq \ell' \leq k'} \exp(e_{i\ell'})}, \alpha_{i'j} = \frac{\exp(e_{i'j})}{\sum_{1 \leq \ell \leq k} \exp(e_{i'\ell})}. \quad (20)$$

These weights are used to find the dynamic embeddings for left node  $v_i$  and right node  $v_{i'}$  as follows,

$$d_i^{ch} = \tanh\left(\sum_{1 \leq j' \leq k'} \alpha_{ij'} \mathbf{W}_{CV'}^T \mathbf{v}_{j'}(t)\right)$$

$$d_{i'}^{ch'} = \tanh\left(\sum_{1 \leq j \leq k} \alpha_{i'j} \mathbf{W}_{CV}^T \mathbf{v}_j(t)\right). \quad (21)$$

Here,  $\mathbf{W}_{CQ}, \mathbf{W}_{CK}, \mathbf{W}_{CV} \in \mathbb{R}^{d \times d}$  are the learnable weights for nodes in the left, and  $\mathbf{W}_{CQ'}, \mathbf{W}_{CK'}, \mathbf{W}_{CV'} \in \mathbb{R}^{d \times d}$  are the learnable weights for nodes in the right.

**SAT.** Given a set of embeddings  $(\{z_1, \dots, z_k\}, \text{with } z_i \in \mathbb{R}^d)$ . The self attention based dynamic embeddings are calculated as follows,

$$e_{ij} = (\mathbf{W}_{SQ}^T z_i(t)) \mathbf{W}_{SK}^T z_j(t), \forall 1 \leq i, j \leq k, i \neq j,$$

$$\alpha_{ij} = \frac{\exp(e_{ij})}{\sum_{1 \leq \ell \leq k, i \neq \ell} \exp(e_{i\ell})}. \quad (22)$$

Datasets	$ \mathcal{V} $	$ \mathcal{E}(T) $	$ \mathcal{H}^r $	$ \mathcal{H}^l $	$T$	$\Delta t(\text{mean})$	$\Delta t(\text{max})$	$\Delta t(\text{min})$	$L(\text{max})$
<b>Enron-Email</b>	183	10,311	1,003	89	99,070.18	6.67	1,589.89	0.0008	3
<b>Twitter</b>	2,130	9,889	1,218	2,321	17,277.80	1.877	41.39	0.18	3
<b>HepTh</b>	451	9,882	8,384	1,352	21,532.70	2.17	275.90	0.0001	1
<b>ML-ArXiv</b>	659	18,558	2,995	17,014	62,741.56	3.38	314.62	0	6

Table 4: Datasets used for Temporal Directed Hypergraphs along with their vital statistics.

Datasets	<i>Datatype</i>	$ \mathcal{V} $	$ \mathcal{E} $	$ \mathcal{H}^r $	$ \mathcal{H}^l $
<b>iAF1260b</b>	metabolic reactions	1668	2084	2010	1985
<b>iJO1366</b>	metabolic reactions	1805	2253	2174	2146
<b>USPTO</b>	organic reactions	16293	11433	6819	6784

Table 5: Datasets used for static Directed Hypergraphs and their vital statistics.

These weights are used to calculate the second dynamic hyperedge embeddings for each node  $v_i$  as,

$$d_i^{sh} = \tanh \left( \sum_{1 \leq j \leq k, i \neq j} \alpha_{ij} \mathbf{W}_{SV}^T z_j(t) \right). \quad (23)$$

Here,  $\mathbf{W}_{SQ}, \mathbf{W}_{SK}, \mathbf{W}_{SV} \in \mathbb{R}^{d \times d}$  are learnable weights.

## C Dataset Descriptions

### C.1 Temporal Datasets

Table 4 shows the statistics of the temporal datasets. Here,  $|\mathcal{V}|$  denotes the number of nodes,  $|\mathcal{E}(T)|$  denotes the number of hyperedges,  $|\mathcal{H}^r|$  denotes the number of unique right hyperedges,  $|\mathcal{H}^l|$  denotes the number of unique left hyperedges,  $T$  is the time span of the dataset, and  $\Delta t(\text{mean}), \Delta t(\text{max}), \Delta t(\text{min})$ , are the mean, maximum and minimum values of inter-event duration, defined as the time difference between two consecutive events.  $T, \Delta t(\text{mean}), \Delta t(\text{max})$ , and  $\Delta t(\text{min})$  are calculated after scaling the original time by the mean value of interevent duration.  $L(\text{max})$  denotes the maximum number of concurrent hyperedges. The following are the temporal-directed hypergraph datasets used to train the model.

**Enron-Email.**<sup>1</sup> This dataset comprises email exchanges between the employees of Enron Corporation. Email addresses are the nodes in the hypergraph. A temporal directed hyperedge is created by using the sender’s address as the left hyperedge, the recipients’ addresses as the right hyperedge, and the time of exchange as the temporal feature. Further, the hyperedge size is restricted to 25, the less frequent nodes are filtered out, and only exchanges involving Enron employees are included.

**Twitter.** [Chodrow and Mellor, 2019] This dataset contains tweets about the aviation industry exchanged between users for 24 hours. Here, directed hyperedge is formed by senders and receivers of a tweet.

**HepTh.** [Gehrke *et al.*, 2003] This is a citation network from ArXiv, initially released as a part of KDD Cup 2003. It covers papers from January 1993 to April 2003 under the HepTh (High Energy Physics Theory) section. The author IDs are the nodes, the directed hyperedge is between the authors of the paper and the cited papers, and the publication time is taken as the time of occurrence. The hyperedge size is restricted to 25, and less frequent nodes are filtered out.

**ML-ArXiv.** This is a citation network created from papers under the Machine Learning categories - "cs.LG," "stat.ML," and "cs.AI" in ArXiv<sup>2</sup>. The definition of the hyperedge is identical to that of the HepTh dataset. All papers published before 2011 are filtered out, and nodes are restricted to authors who have published more than 20 papers during this period. Citations between these papers are considered to create a directed hyperedge.

### C.2 Static Datasets

Table 5 shows the statistics of the static datasets. Here, *Datatype* denotes the type of the data,  $|\mathcal{V}|$  denotes the number of nodes,  $|\mathcal{E}|$  denotes the number of hyperedges,  $|\mathcal{H}^r|$  denotes the number of unique right hyperedges, and  $|\mathcal{H}^l|$  denotes the number of unique left hyperedges. Following are the static directed hypergraph datasets used to test the performance of directed hyperedge link predictor in Section 4 against previous state-of-the-art architectures.

**iAF1260b** This is a metabolic reaction dataset from BiGG Models<sup>3</sup>. It is a knowledge-base of genome-scale metabolic network reconstructions.

**iJO1366** Similar to the above, a metabolic reaction dataset from BiGG Models.

**USPTO** This dataset consists of reactions from USPTO-granted patents [Lowe, ]. This dataset has been processed and prepared to consist of organic reactions created using a subset of chemical substances containing only carbon, hydrogen, nitrogen, oxygen, phosphorous, and sulfur.

<sup>1</sup><http://www.cs.cmu.edu/enron/>

<sup>2</sup>[https://arxiv.org/help/bulk\\_data](https://arxiv.org/help/bulk_data)

<sup>3</sup><http://bigg.ucsd.edu/>

## D Baseline Models

### D.1 Pairwise Models

**TGN.** [Rossi *et al.*, 2020] This is the state-of-the-art model for pairwise link forecasting in dynamic networks. Here, a memory module is used to capture the long-term interaction information and a temporal attention layer [da Xu *et al.*, 2020] to learn dynamic node embeddings. To adapt this model to predict higher-order interactions, we use clique expansion to convert hyperedge to pairwise edges. For example given a directed hyperedge event  $(\{v_1, \dots, v_k\}, \{v_{1'}, \dots, v_{k'}\})$  at time  $t$ , we create two different sets of pairwise interactions using clique expansions; i)  $\{((v_1, v_2), t), \dots, (v_{k-1}, v_k), t)\}$  using pairwise expansion of right hyperedge and ii)  $\{((v_1, v_{2'}), t), \dots, (v_{k-1'}, v_{k'}), t)\}$  using cross edges between left and right hyperedge. We use separate link prediction models to estimate the probability of each type of edge.

**GAT.** The Graph Attention Network (GAT) [Veličković *et al.*, 2018] model uses the attention mechanism to give importance scores for different neighbors for each node, allowing it to focus on the most informative parts of the graph. To adapt GAT to hypergraphs, we used a similar approach as TGAT but removed the time stamp as GAT does not consider temporal features of the graph. For predicting an edge at time  $t$ , we construct a pairwise graph with all edges that occurred before time  $t$ .

### D.2 Hyperedge Models

**HGDHE, HGBHDE.** [Gracious and Dukkupati, 2023] These models use a temporal point process framework for modeling interactions. For each possible hyperedge, a TPP is defined with its intensity as a function of the dynamic node embedding,

$$\lambda(h_{n+1,j}) = \text{softplus}(f(\{\mathbf{v}_i(t)\}_{v_i \in h_{n+1,j}})).$$

So, the likelihood for event  $(e_{n+1}, t_{n+1})$  given  $\mathcal{E}(t_n)$  can be written as,

$$\begin{aligned} p((e_{n+1}, t_{n+1}) | \mathcal{E}(t_n)) &= \\ &\prod_{h_{n+1,j} \in e_{n+1}} \lambda_{h_{n+1,j}}(t_{n+1}) \\ &\exp\left(-\sum_{h \in \mathcal{H}} \int_{t_n}^{t_{n+1}} \lambda_h(\tau) d\tau\right). \end{aligned} \quad (24)$$

Here,  $\mathcal{H}$  is all possible hyperedges. The loss is calculated over all events as follows,

$$\begin{aligned} \mathcal{L} &= \sum_{n=0}^{N-1} \left( \sum_{h_{n+1,m} \in e_{n+1}} \log \lambda_{h_{n+1,m}}(t_{n+1}) \right. \\ &\quad \left. - \sum_{h \in \mathcal{H}} \int_{t_n}^{t_{n+1}} \lambda_h(\tau) d\tau \right). \end{aligned} \quad (25)$$

However, these models are not scalable as they use each hyperedge as separate events, and the number of possible hyperedges is exponential with respect to the number of nodes, so these models cannot be applied to real-world networks.

HGDHE is used for modeling undirected hyperedge with HyperSANN [Zhang *et al.*, 2020] decoder for  $f(\cdot)$  with dynamic representation learned as a function of time and historical interactions. When a node is involved in an interaction it update the embeddings based on the features of the interaction using a recurrent neural network architecture. These updated embeddings are used for dynamic embedding calculation with Hypergraph convolution layer [Bai *et al.*, 2021] and Fourier feature [da Xu *et al.*, 2020] time features to model the evolution node during the interevent time. HGBDHE is used for modeling bipartite hyperedges with CATSETMAT [Sharma *et al.*, 2021] decoder for hyperedge prediction, but we use them for modeling directed hyperedges. Here, left and right hyperedge have different dynamic embeddings but follow the same architecture of HGDHE.

To predict the duration for future interaction for these models, we have to calculate the expected time  $t$  with respect to the event probability distribution as shown below,

$$\begin{aligned} \hat{t} &= \int_{t_n^p}^{\infty} (\tau - t_n) p_h(\tau) d\tau \\ p_h(t) &= \lambda_h(t) \exp\left(-\int_{t_n}^{\infty} \lambda_h(\tau) d\tau\right). \end{aligned} \quad (26)$$

For forecasting type of interaction a time  $t$  can be done by finding the  $h_i$  with the maximum conditional intensity value, as shown below,

$$\hat{h} = \arg \max_{h_i} \lambda_{h_i}(t). \quad (27)$$